

Pre-research on arithmetic for facing control of segmented-mirror in LAMOST

Hanjie Miao^{1,2}, Yongjun Qi¹

1. Nanjing Institute of Astronomical Optics & Technology, National Astronomical Observatories, CAS, 188 Bancang Street, Nanjing City, 210042, P.R.China
2. Graduate School of the Chinese Academy of Sciences, Beijing 100049

ABSTRACT

Main mirror in LAMOST is a spherical mirror with 4 meters effective aperture, it is assembled by 37 hexagonal segments, and the orientations of these segments were adjusted by actuators to achieve optical co-focal status. Arithmetic for facing control of segmented-mirror was pre-researched in this paper, based on present condition in LAMOST. To maintain the main mirror in a facing figure and preserve it during the track is the core of this control. To achieve the facing figure, the unique method in segmented-mirror technology nowadays is that sensors working with actuators to form closed loop. Firstly, relationship between the measurement results of sensors and the movements of actuators was calculated and the figure control equation set was founded. Secondly, the characteristic of the coefficient matrix of this equation set was analyzed. Finally, several methods to solve this equation system were comprehensively analyzed. Damped Least-Squares Solution (DLS) was selected as the best for this paper, and this method was programmed to apply on the experiment of sub system, finer result was got. Petal-effect in the experiment was noticed, analysis was given to show the control of whole main mirror would get rid of petal-effect.

Key words: segmented-mirror, facing control, sensor, equation set, DLS, petal-effect

1. INTRODUCTION

In astronomy today, astronomical telescopes are being made with increasingly larger apertures. However, our ability to improve the apertures by means of molding larger-aperture monolithic mirrors has reached its limit. It is very difficult to overcome the financial and technological difficulties associated with building a traditional telescope with larger than 8-m aperture.

Active Optics makes it possible for us to build larger telescopes. LAMOST (Large Sky Area Multi-Object Fiber Spectroscopy Telescope) is based on segmented-mirror active optics. LAMOST consists of a reflecting Schmidt corrector MA at the northern end, a spherical primary mirror MB at the southern end and a focal plane in the middle. Both the primary mirror and the focal plane are fixed on their ground bases, and the reflecting corrector tracks the motion of celestial objects.

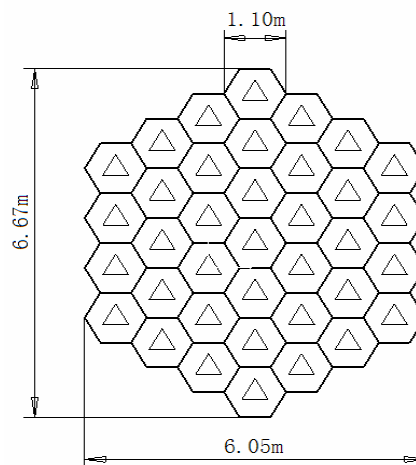


Fig 1. Configuration of the primary mirror (MB) of LAMOST

Shack-Hartmann equipment is used to detect the orientations of mirror segments to obtain the ideal mirror figure that we require in LAMOST. However, the time it takes is too long. So, we use displacement sensors to maintain the facing of main mirror. Translating the sensor information into the desired actuator motions is the task of this control algorithm. This mathematical problem is closely related to the geometry of the sensor–actuator array and the solution to calculate equation set, which are both discussed in this paper. At the end, a successful sub system experiment and the analysis based on the result of experiment are given.

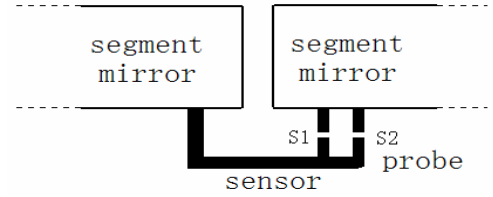


Fig 2. Configuration of the displacement sensor used in LAMOST

Displacement sensor used in this pre-research is shown in Fig2. Each sensor includes two probes (S1, S2). As the two have similar geometry relationship with actuators, we only have to analyze one of them.

2. ESTABLISHMENT OF FIGURECONTROL EQUATION SET

Although the segments are actually located on a large spherical surface, the sensor–actuator relations can be described in plane geometry with sufficient accuracy with respect to the relatively small curvature of the primary mirror.

Assume that side length of each hexagonal segment is A , the radius of the circum circle of the triangle formed by the three actuators under a segment is R , the distance between the point of intersection (made of a sensor and the side of hexagonal segment it across) and the nearer endpoint of the side of hexagonal is L , the distance between the probe and the point of intersection mentioned above is L_1 , the distance between the borders of two adjacent segments is G . The geometry relationship between the changes of S_1 , S_2 and the displacements of D_1 , D_2 ,

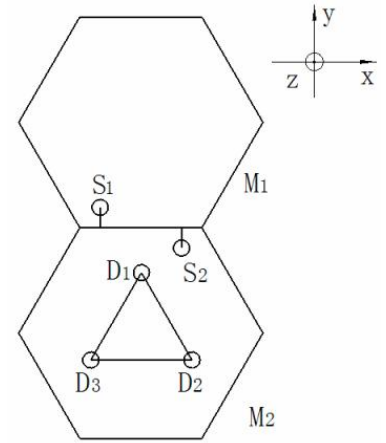


Fig 3. Sensor–actuator geometrical relationships

D_3 shown in Fig3 is discussed below (the angle of view of fig3 is behind segment, the displacement of D to push segment away from bracket is defined positive):

Firstly, the relationship between D_1 and S_1 is linear^[1]. So, we can get the linear coefficients by seeing about special situation. Assume that D_2 and D_3 is locked in zero, it's obviously that:

$$\frac{S_1}{D_1} = \alpha = -\frac{\sqrt{3}A + R + 2L_1 + 2G}{3R} \quad (2.1)$$

$$\frac{S_2}{D_1} = \beta = \frac{\sqrt{3}A + R - 2L_1}{3R} \quad (2.2)$$

In like manner:

$$\frac{S_1}{D_2} = \gamma = \frac{\sqrt{3}A - R - \sqrt{3}L + L_1 + G}{3R} \quad (2.3)$$

$$\frac{S_2}{D_2} = \delta = \frac{R - \sqrt{3}L + L_1}{3R} \quad (2.4)$$

$$\frac{S_1}{D_3} = \varepsilon = -\frac{R - \sqrt{3}L - L_1 - G}{3R} \quad (2.5)$$

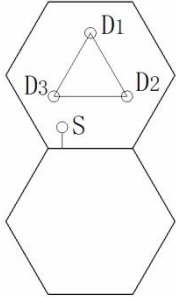
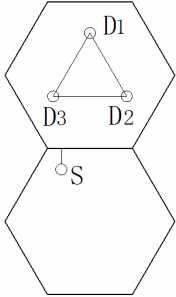
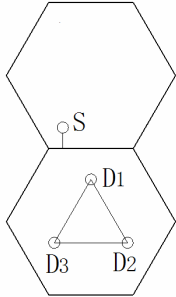
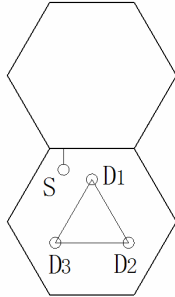
$$\frac{S_2}{D_3} = \varsigma = -\frac{\sqrt{3}A - R - \sqrt{3}L - L_1}{3R} \quad (2.6)$$

According to the linear coefficients above, we can get the figure control equation set:

$$\begin{bmatrix} \alpha & \gamma & \varepsilon \\ \beta & \delta & \varsigma \end{bmatrix} \begin{bmatrix} D_1 \\ D_2 \\ D_3 \end{bmatrix} = \begin{bmatrix} S_1 \\ S_2 \end{bmatrix} \quad (2.7)$$

The figure control equation set of the whole main mirror is generalized from (2.7). According to Fig1, each sensor only related to 6 actuators (behind the 2 segments the sensor across). The geometries between one single sensor and one single triangle formed by the three actuators under a segment can be concluded in 4 types:

Tab1. Sensor-Actuator Geometries

I	II	III	IV
			

We get the figure control equation set by the linear coefficients analyzed for each geometries type. The equation set is too large to be shown in this paper, so it is left out.

3. SOLUTION OF FIGURECONTROL EQUATION SET

The solution of figure control is a core problem in active optics. Several methods are given below:

3.1 Least-Squares Solution (LS)

Over determined equation set $Ax = b$, if $x^* \in R^n$ satisfies

$$\min_{x \in R^n} \|b - Ax\|_2^2 = \|b - Ax^*\|_2^2 \quad (3.1)$$

x^* is called the answer of Least-Squares to this equation set.

Least-Squares solutions can be grouped in two types: direct solution and iterative solution. Direct solution is able to get the accurate answer in theory, but actually, because of the rounding errors, the answer is approximate as well. Iterative solution use some limit condition to get close to the exact answer step by step. Iterative solution takes less store space than direct solution, but it takes too much time to be used in LAMOST. So, we only consider direct solution.

Singular-value decomposition (SVD) algorithm^[3] algorithm used by Mast and Nelson in 1982^[2] is one kind of direct solution.

3.2 Total Least-Squares Solution (TLS)

Over determined equation set $Ax = b$ (3.2)

The exact linear system described by (3.2) $x = A^\dagger b$ (3.3)

(3.3) is consistent. (3.2) is inconsistent because of the errors in A and b.

If we consider (3.2) as consistent equation set, the answer to (3.2) is equal to the answer of:

$$Ax = AA^\dagger b \quad (3.4)$$

The answer is:

$$x = A^\dagger + (I - A^\dagger A)Z \quad Z \in C^{n \times d} \quad (3.5)$$

So, the Least-Squares solution of (3.2) is equal to the solution of (3.4). But, it takes a situation as acquiescently that there is no error in A, errors are all in b. TLS is developed to find new consistent equation set:

$$\hat{A}x = \hat{b} \quad (3.6)$$

\hat{A} in (3.6) may be changed a lot from A in (3.2) and \hat{b} may be just changed a little from b. As b includes more error than A in the figure control equation set, we choose LS instead of TLS.

3.3 Damped Least-Squares Solution (DLS)

There are errors in sensors, so if we take sensors' data into the equation set we may get larger actuator motions than what we really want. The situation may be even worse if we only use a few segments to do experiments. We can get better actuator motions with the help of DLS.

When we use just a few segments, normal equation set of the figure control equation set is morbid, the condition number of this equation set is too bad to get a static answer. DLS changes the coefficient matrix of normal equation set from $A^T A$ into $A^T A + \lambda I$ (I is $n \times n$ identity matrix, λ is called damped gene, it is a proper positive number). The condition number of this new matrix is better.

Assume that λ_N is the biggest eigenvalue of $A^T A$ and λ_1 is the smallest one.

The condition number of $A^T A$ is: λ_N / λ_1

The condition number of $A^T A + \lambda I$ is: $(\lambda_N + \lambda) / (\lambda_1 + \lambda)$

The aim of DLS is not only to get the smallest fitting variance, but also to get the smallest change. Change gets bigger when λ gets smaller. DLS changes to LS when $\lambda = 0$.

4. SUB SYSTEM EXPERIMENT

Sub system is shown in Fig4. It includes 3 segments (M1~M3). Actuators behind M1 are locked, 6 actuators behind M2 and M3 are signed with big circles, 12 probes of 6 sensors are signed with small circles.

The coefficients matrix of figure control equation set was made in the method shown in section2.

We measured coefficients matrix by moving one actuator a time with the others locked. Because the bracket cannot transfer the actuator displacement 100% to the mirror when the displacement is very small, there must be some error in the measured coefficients matrix. We found that the proportion of the coefficients of two probes in every sensor is the same between theory and practicality.

We firstly tried SVD chosen by Mast and Nelson. However, the figure of mirror got worse when the actuators were modulated. As analyzed in 3.3, we chose DLS for sub system experiment.

The key of DLS is the choice of λ . The smaller λ we choose, the quicker the answer to the equation set converge, and also the easier the figure of mirror goes bad. When $\lambda = 0$, DLS is equal to LS. So, λ should be big enough to make sure the figure of mirror goes better and also be small enough to make sure the control goes as quickly as possible.

The program was designed in the flow below to choose proper λ and take displacement to actuators.

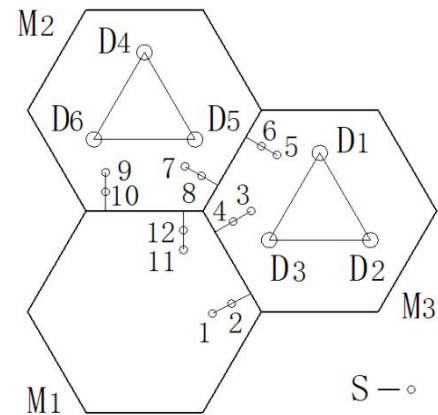
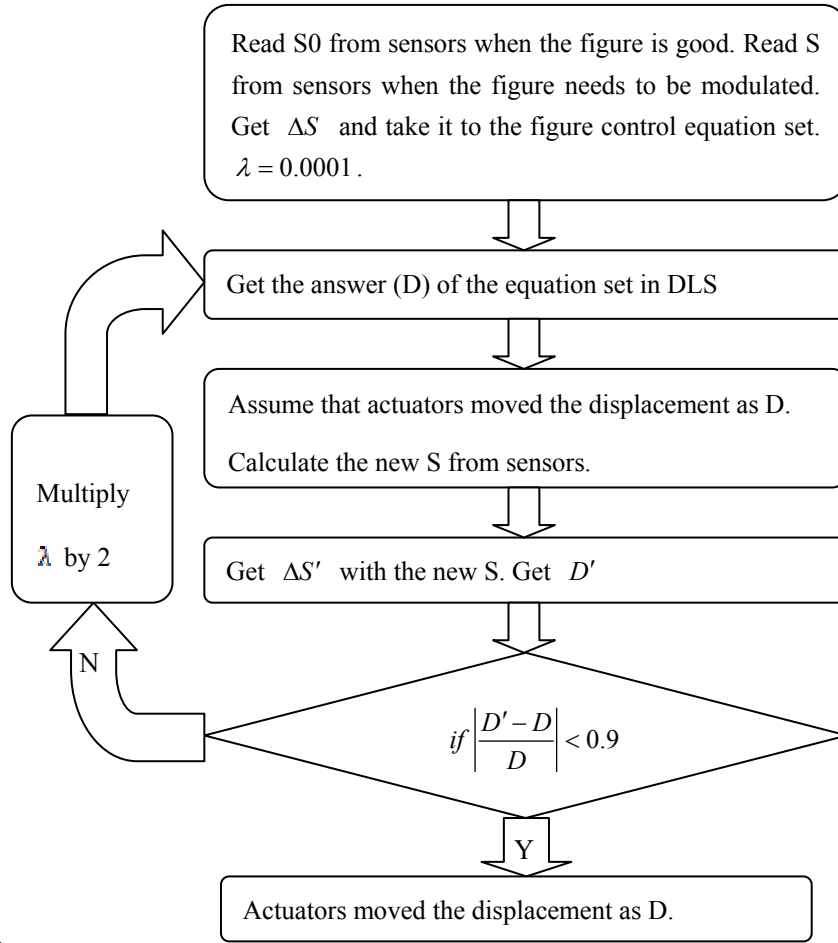


Fig 4. Configuration of the sub system



“if $\left| \frac{D' - D}{D} \right| < 0.9$ ” in the flow was used to choose the proper λ . “0.9” is confirmed after lots of simulation. The

program worked well in the experiment: Actuators were drive away in 10 microns to destroy the good figure. The figure could be gotten back in 4 times of modulate at most.

The sensor used in LAMOST includes 2 probes (fig2). One gets beyond the borderline 6mm, the other 26mm. If there is no error in the sensor, information of angle could be given by these 2 probes. But petal-effect was still found in the experiment because of the error. Each probe includes error in $\pm 15nm$. The error of figure brought by one single sensor can be calculated as:

$$\tan^{-1} \frac{15 - (-15)}{(26 - 6) \times 10^6} = 0.3 \text{ arc sec} \quad (4.1)$$

Because the errors in sensor do not always get the high-point, and the error of figure brought by many sensors could be counteracted, the final effect should be much less. Take sub system examination for example: error of figure brought by sensors of 5+6 and 7+8 is in the same direction, they will be counteracted by themselves. The situation is that although there was petal-effect in the experiment, the error of figure control was limited in 0.05 arc-second. So, it is concluded for LAMOST that the more sensors, the less petal-effect.

In other way, petal-effect could be limited by the native figure in LAMOST (fig 5). Consider the first ring of segments and the middle segment, petal-effect could be happen because the sensors in the overstriking borderline between them could only limit the height instead of the angle. Consider the first and the second ring of segments, the two cross overstriking borderline between them belongs to one segment in the second ring, they could only limit the height instead of the angle separately as well. However they could limit the single segment in the second ring together. As a result, there is no petal-effect between the first and the second ring. In the same manner, there is no petal-effect between the second and the third ring. So petal-effect is only between the first ring and the middle segment. If there is a small angle between the first ring and the middle segment, actuators in the outer rings should move a lot to keep the same angle with the first ring. This big movement will not be picked out based on the theory of DLS, because the displacements of actuators matching petal-effect get bigger change than the displacement without petal-effect.

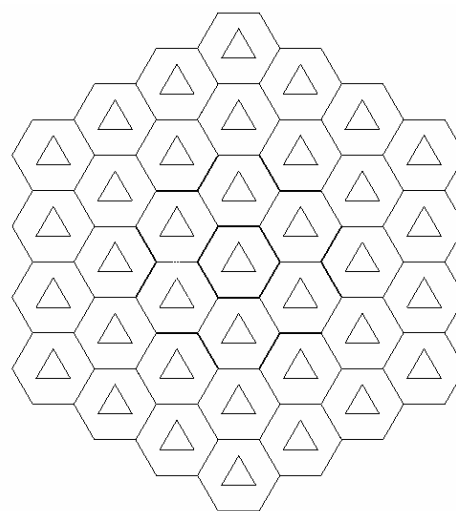


Fig 5. Analysis of petal-effort

In conclude, petal-effect would be too small to be noticed in the control of main mirror.

5. CONCLUSION

Figure control algorithm for LAMOST was pre-researched in this paper, including the establishment and solution of figure control equation set. Four typical sensor-actuator geometries were concluded. Three typical solutions were concluded and DLS was selected as the best for this paper.

The algorithm worked well in the sub system experiment. Petal-effect in the experiment was noticed, analysis was given to show the control of whole main mirror would get rid of petal-effect.

References

- [1] Weiyao Z., "The figure control of large segmented mirror telescope" Master's thesis (Chinese Academy of Sciences, Nanjing, China, 1996).
- [2] Mast, T. S. and Nelson, J. E., "Figure control for a fully segmented telescope mirror" Appl. Opt. 21, 2631–2641 (1982).
- [3] Golub, G. H. and Reinsch, C., " Singular value decomposition and least squares solutions," Number. Math. 14, 403–420(1970).
- [4] Javier Castro, F. and Juan C. Gonzalez, "Development of a test rig for the active control of a segmented mirror support system" SPIE Vol. 2871 /343 - 351 (1997).
- [5] John R., Drew H., "Primary mirror figure maintenance of the Hobby-Eberly Telescope using the Segment Alignment Maintenance System" SPIE Vol. 4837 (2003)

- [6] John A. B., Mark T. A., "Development of the Segment Alignment Maintenance System (SAMS) for the Hobby-Eberly Telescope" SPIE Vol. 4003 (2000).
- [7] Pierre De Fonseca, Paul Sas, Hendrik Van Brussel, "Optimization methods for choosing sensor and actuator locations in an actively controlled double-panel partition" SPIE Vol. 3041 (1997).
- [8] Weiyao Z., "Generalized figure-control algorithm for large segmented telescope mirrors" Optical Society of America Vol. 18,638-649 (2001)